NASA TT F-10,025

INFRARED SPECTROPHOTOMETRY OF THE MOON AND THE GALILEAN SATELLITES OF JUPITER

V.I.Moroz

Translation of "Opyt infrakrasnoy spektrofotometrii sputnikov: Luna i galileyevskiye sputniki Yupitera". Astronomicheskiy Zhurnal, Vol.42, No.6, pp.1287-1295, 1965.

NATIONAL AERONAUTICS AND SPACE ADMINISTRATION
WASHINGTON MARCH 1966

INFRARED SPECTROPHOTOMETRY OF THE MOON AND THE GALILEAN SATELLITES OF JUPITER

*/1287

V.I.Moroz

Spectra of selected areas of the Moon have been obtained with a prismatic infrared spectrometer and the 125 cm reflector. The spectral region 0.8 - 3.8 μ with a dispersion $\lambda/\Delta\lambda$ of 20 (at 1.6 μ) to 80 (at 3.4 μ) was studied. The increase of albedo with wavelength, at least up to 2.2 μ, is approximately identical for all the investigated areas, which include maria, continents and bright craters. Among terrestrial materials volcanic ash and slag show a similar dependence of albedo on wavelength. The contribution of thermal radiation is essential in the 3 - 4 μ region. The temperature of the subsolar point derived from the thermal excess is 395°. The same spectrometer and the 125 cm and 260 cm reflectors were used for observations of the spectra of the Galilean satellites in the 0.8 - 2.5 μ region. The recordings of Europa and Ganymede show details characteristic of the reflection spectrum of a snow layer.

Diffraction and prismatic spectra of the moon were recorded by the author in 1961 - 1964 at numerous occasions, as comparison spectra during observations of the planets (Bibl.1, 2, 3). On October 2 - 3, 1963 during full moon, a special series of observations was carried out on the 125-cm reflector of the Southern Station of the GAISh (Shternberg State Astron. Institute) in the

---

* Numbers in the margin indicate pagination in the original foreign text.

0.8 - 3.8 μ spectral region, using a prismatic infrared spectrophotometer and a 0.5 × 0.5-mm lead sulfide photoconductive detector cooled by liquid nitrogen. The purpose of these observations was to compare the spectrophotometric properties of selected areas of the lunar surface in the infrared region. The width

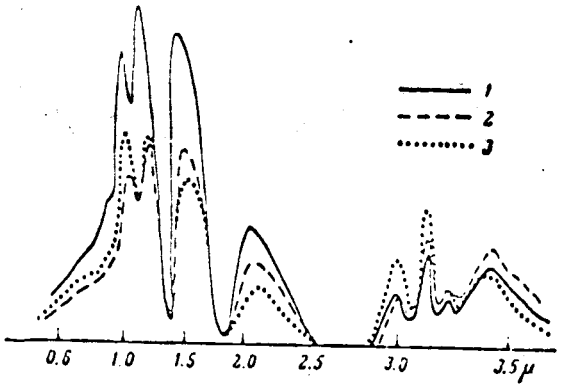

Fig.1 Lunar Spectrum in the 0.6 - 3.6 μ Region (October 2-3, 1963)
1 - Tycho; 2 - Mare Serenitatis; 3 - Comparison spectrum (sun). ZTE, prism spectrometer (LiF), slits 1 mm ($\Delta\lambda \simeq 0.09$ μ), recording speed 70 Å/sec (at 1.6 μ), τ = 2.2 sec. Recording of the 2.8 - 3.6 μ region was enlarged by a factor of 9 for the moon and by 60 for the sun.

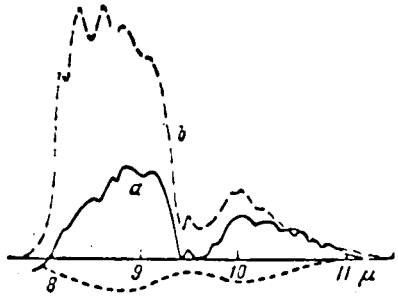

Fig.2 Lunar Spectrum in the 8 - 11 μ Region, Average of Four Recordings (June 30, 1964)
ZTE, prism spectrometer (NaCl), slits 1 mm ($\Delta\lambda \simeq 0.2$ μ):
a - Moon; b - Modulator emission; c - Sun

of the entrance and exit slits was 1 mm, which corresponds to a spectral resolution of about 0.09 μ close to 1.6 μ, and of 0.045 μ close to 3.5 μ; the height of the entrance slit was 2 mm. The angular dimensions of the entrance slit were

11 × 22". Samples of the original recordings are shown in Fig.1. The 3 - 4 μ region was recorded at a magnification 9.1 times greater than the 0.7 - 2.5 μ region. These observations were carried out with a LiF prism. Furthermore, in May - June, 1964 we obtained test recordings in the 8 - 11 μ region (Fig.2), using a NaCl prism and a photoconductive detector made of germanium alloyed with zinc and cooled by solid nitrogen. In all cases a fluorite collector was used. The guiding accuracy was 2 - 3".

TABLE 1 /1288

Object	Reading at 1.6 μ	Ratio of Reading at Given Wavelength to Reading at 1.6 μ							Zenith Distance
		0.80	1.1	1.26	1.60	2.2	3.0	3.15	3.4	
Tycho	122	0.32	0.87	1.11	1.00	0.40	0.021	0.032	0.023	48°
Bright matter close to Tycho	117	0.34	1.03	1.15	1.00	0.42	0.028	0.031	0.025	48
Copernicus	86	0.31	0.95	1.03	1.00	0.43	0.017	0.034	0.028	49
Caucasus	80	0.28	0.95	1.10	1.00	0.43	0.022	0.040	0.032	47
Weiss	69	0.30	0.91	1.10	1.00	0.41	0.033	0.041	0.054	47
Mare Serenitatis	56	0.28	0.87	1.03	1.00	0.41	0.030	0.051	0.054	48
Mare Nubium	59	0.28	0.87	1.03	1.00	0.42	0.32	--	0.053	59
Sun		0.41	1.30	1.27	1.00	0.35	0.0088	0.0137	0.0076	60

On October 2 - 3, we observed seven areas in all which are listed in Table 1. Table 1 shows the readings at 1.6 μ and the magnitude of K_λ which is the ratio of the readings at a given wavelength to the reading at 1.6 μ. We selected those points in the spectrum at which the effect of telluric absorption bands was minimal. All observations were carried out in a narrow range of air masses; the corrections for transparency of the atmosphere were minimal at the selected points of the spectrum, when comparing the various areas observed at different times, and there they were not introduced. It was essential to have the observations made during full moon, when the brightness of the various points of the disk was proportional to the albedo (Bibl.4). The values of K_λ

for the sun are shown in the last row of Table 1.

An examination of the data in Table 1 yields the following conclusions:

1) The brightness (and thus also the albedo) of the brightest areas is about twice as great as that of the darkest areas. The same is true for the visible spectrum region (Bibl.5);

2) The dependence of K_λ in the 0.8 - 2.2 μ region is almost the same for all of the investigated areas: the bright matter of the rays and maria and the dark and bright craters have the same color in the 0.8 - 2.2 μ region; they differ only in brightness. It is known that in the 0.3 - 0.7 μ region the color

/1289

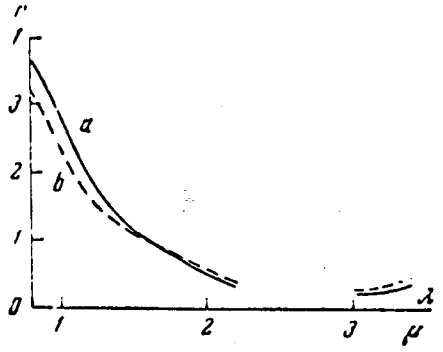

Fig.3 Relative Energy Distribution in the Lunar Spectrum in the 0.8 - 3.4 μ Region
a - Bright craters (Tycho, bright matter next to Tycho); b - Maria (Mare Serenitatis, Mare Nubium).

differences between details of the lunar surface are slight. Our observations showed that this property is retained up to 2.2 μ. A comparison with the values of K_λ, obtained for the sun, indicates that the albedo increases with wavelength in the 0.8 - 2.2 μ region. It is known that the variation in albedo with wavelength in the 0.3 - 0.8 μ region has the same character. In the 0.8 - 1.6 μ region, both Mare Serenitatis and Mare Nubium are somewhat redder than the five other brighter areas. However, the difference is slight, and the limited nature of the evidence did not permit us to judge whether this is typical.

3) In the 3.0 - 3.4 μ region, the values of K_λ for the various areas differ substantially, increasing on the average with a decrease in albedo. Figure 3 shows the relative energy distribution in the lunar spectrum. It is apparent that, in the 3.0 - 3.4 μ region, thermal radiation of the moon already furnishes a notable contribution. The temperature of the dark areas is higher, so that the values of K_λ in the 3.0 - 3.4 μ region are also greater for these.

TABLE 2

λ	K_λ, Average for all Areas	$K_\lambda/K_{\lambda\odot}$	p			λ	K_λ, Average for all Areas	$K_\lambda/K_{\lambda\odot}$	p		
			Average	Maria	Bright Matter of the Rays and Craters with a Bright Floor				Average	Maria	Bright Matter of the Rays and Craters with a Bright Floor
0.80	0.30	0.73	0.17	0.11	0.23	1.60	1.00	1.00	0.23	0.15	0.31
1.10	0.91	0.72	0.17	0.11	0.23	2.20	0.42	1.16	0.27	0.18	0.36
1.25	1.07	0.85	0.20	0.13	0.27						

Table 2 shows the average dependence of K_λ for all investigated areas and the values of the average geometric albedo calculated for the same wavelengths, assuming p = 0.17 at 0.8 μ. This value was obtained by Harris (Bibl.6). The same author gives the values of the geometric albedo for maria (p_m) and bright craters (p_{cr}) calculated on the assumption that

$$\frac{p_m}{p_{av}} = 0.65; \tag{1}$$

$$\frac{p_{cr}}{p_{av}} = 1.30. \tag{2}$$

The same relationships were obtained by N.N.Sytinskaya for the visible spectrum region (Bibl.5). Since the color of the maria and of the continents apparently is almost identical in the 0.3 - 2.2 μ region, we can use eqs.(1) and (2) in this entire interval.

Kuprevich (Bibl.7), on the basis of television photographs of the moon ob-

tained in the 1 - 2 μ region, drew the conclusion that the bright matter of the rays has an energy distribution in the infrared region of the spectrum, which substantially differs from that of the other details. Our spectroscopic observations do not bear this out.

/1290

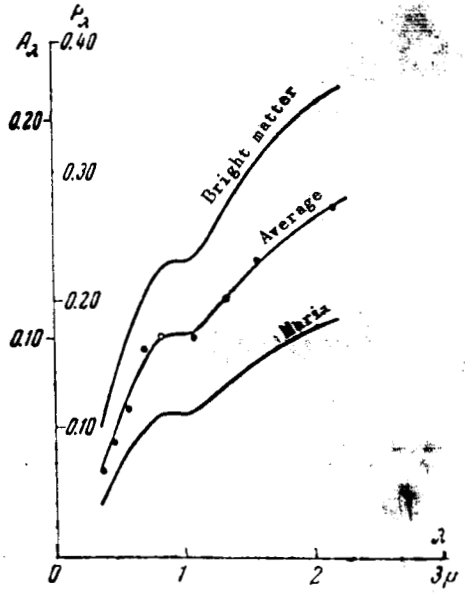

Fig.4 Geometric Albedo of the Moon as a Function of Wavelength

Figure 4 shows the dependence of the geometric albedo of the moon on the wavelength, over a wide range from 0.35 to 2.2 μ [in the 0.35 - 0.8 μ region, the data by Harris were used (Bibl.6)]. It is of interest to compare this curve with the spectral dependence of the reflection coefficient of terrestrial rocks. We find that volcanic lavas, basalt, and tuff give approximately a neutral dependence of the brightness coefficient on wavelength in the 1 - 2.5 μ region. Volcanic ash and scoria exhibit a systematic increase of the brightness coefficient with wavelength. The characteristic absorption component at 1 μ, which lies in the lunar spectrum (Fig.4), is duplicated in the spectrum of volcanic ash and scoria (Fig.5). It is curious that the polarization curves of the moon

coincide well with those of volcanic ash (Bibl.8). Similar comparisons have repeatedly been made in the past, based on the colorimetric and spectrophotometric data in the visible and photographic regions of the spectrum [see, for example, (Bibl.9)]. Broadening of the spectral range substantially enhances this method but its reliability is not high, even in this case. First, identification of the chemical composition of materials in the solid phase can rarely be done without ambiguity from reflection spectra in the visible and near-infrared regions. Very often, different materials produce similar spectra. The narrower the investigated region, the greater the probability of a chance coincidence. Second, in observations of the moon, averaging over large areas takes

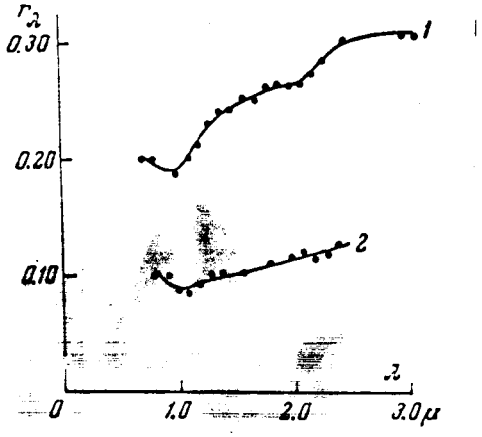

Fig.5 Brightness Coefficient of Volcanic Ash as a Function of Wavelength
1 - Light-colored ash from the Apokhonchich lava flow; 2 - Volcanic sand from Klyuchevskaya volcano. The brightness coefficients are measured relative to a magnesium screen.

place (in our case, about 40 × 80 km), whereas in the laboratory small specimens are used. Third, the conditions to which lunar and terrestrial rocks are subject differ widely. Lunar rocks are exposed to corpuscular fluxes, ultraviolet radiation from the sun, and extreme temperature fluctuations.

A more or less reliable identification of the chemical nature of crystal-

line materials can be made on the basis of the position of the intense bands corresponding to the fundamental frequencies of the natural oscillations of the crystal lattice. At fundamental frequencies, crystals produce a sharp increase of the reflection factor (and thus a decrease of the emission coefficient) in an interval of 1 - 2 μ width. An absorption band should be observed at this location in the emission spectrum. In the case of SiO_2, this band is at 9 μ (Bibl.10). Van Tassel and Salisbury (Bibl.11) demonstrated, however, that /1291 the quartz band at 9 μ almost disappears when the material is in a finely divided phase (particles measuring several microns).

The emission spectrum of the moon in the 8 - 11 μ region (see Fig.2) shows no absorption components. Since it cannot per se be assumed that there are no silicate rocks on the moon, the only possible conclusion is that the surface layer of the moon, responsible for the infrared thermal radiation, has a finely crushed structure of the dust or pumice type. As is known, estimates of the thermal conductivity of the lunar rocks independently indicate such structural characteristics of the surface layer (Bibl.12, 13).

The integrated spherical albedo of the moon was calculated by means of the curves in Fig.4. Since the various areas of the moon differed little in color, the integrated albedo is proportional to the monochromatic. For the brightest areas it is 0.116; for the maria, 0.058; and on the average for the moon, 0.086. The phase integral for all wavelengths was taken as q = 0.585 (Bibl.6). Table 3 gives the values of the integrated spherical albedo, calculated separately for each of the observed areas, and the corresponding theoretical temperatures

$$T_{theor} = \sqrt[4]{\frac{E(1 - A_i)}{\sigma\varepsilon}}\cos\theta, \qquad (3)$$

where E is the solar constant; σ is the Stefan-Boltzmann constant; A_i is the

integrated albedo; ϵ is the emission coefficient (average, taken as $\epsilon = 0.85$); θ is the angle between the normal to the surface and the direction to the sun.

/1292

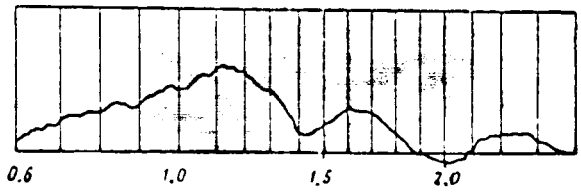

Fig.6 Spectrum of Ganymede in the 0.7 - 2.5 μ Region
(Single Recording)
ZTE, October 3, 1963, prism spectrometer (LiF),
spectral width of the exit slit $\Delta\lambda$ = 0.18 μ (at 1.6 μ),
recording speed 35 Å/sec, τ = 20 sec, z = 50 - 52°

The lunar temperature has been repeatedly determined from the average brightness of the thermal radiation in an 8 - 13 μ window (Bibl.14, 15). For the same purpose, we can use the brightness of the thermal radiation in a 3 - 4 μ window. Here, reflected radiation makes some contribution, but in that case the brightness depends on the temperature to a much greater extent than in the 8 - 13 μ region, since the Wien segment of the energy distribution curve is used. The brightness of the thermal radiation at a wavelength of 3.4 μ can be obtained from our measurements by means of the formula

$$B_{3.4} = \left(\frac{K_{\lambda}}{K_{\lambda\odot}} p_{1.6} - \right) \frac{E}{\pi}, \qquad (4)$$

where p_{λ_e} is the value of the geometric albedo extrapolated from the shorter wave portion of the spectrum; $p_{1.6}$ is the geometric albedo at 1.6 μ; K_{λ} and K_{λ} are the values of K_{λ} for the moon and for the sun.

In the region where thermal radiation is absent, the quantity

$$p_{\lambda}' = \frac{K_{\lambda}}{K_{\lambda\odot}} p_{1.6} \qquad (5)$$

represents the geometric albedo. In the region where the thermal radiation

reaches a noticeable magnitude, we have

$$p_\lambda' > p_\lambda.$$

Table 3 gives the values of p_λ' and p_e calculated for λ 3.4 μ.

The values of p_e vary from 0.20 to 0.40, and those of p' from 0.94 to 1.21. The third column of Table 3 gives the values of $A_e = p_e q$ which is the extrapolated spherical albedo. By means of the values of p' and p_e, we calculated the brightness $B_{3.4}$ and the brightness temperature T_B from Planck's equation

$$B(T) = B_{3.4}$$

and the true T_{tr} by the formula

$$B(T_{tr}) = \frac{B_{3.4}}{\varepsilon}.$$

We assumed that $\varepsilon_{3.4} = 1 - A_e$.

TABLE 3 /1292

Object	p_e	A_e	p'	$B_{3.4}$ w · cm^{-2} · μ^{-1}	T_B deg	$B_{3.4}(1-A_e)$	T_{tr}	A_i	$\frac{1-A_i}{\varepsilon}$	cos θ	T_{theor}
Tycho	0.40	0.23	0.94	$2.9 \cdot 10^{-4}$	368	$3.8 \cdot 10^{-4}$	378	0.116	1.05	0.52	384
Bright matter close to Tycho	0.40	0.23	0.95	$2.9 \cdot 10^{-4}$	368	$3.8 \cdot 10^{-4}$	378	0.116	1.05	0.52	[illegible]
Copernicus	0.40	0.23	1.12	$3.4 \cdot 10^{-4}$	373	$4.4 \cdot 10^{-4}$	384	0.116	1.05	0.90	388
Caucasus	0.27	0.16	1.26	$5.3 \cdot 10^{-4}$	389	$6.3 \cdot 10^{-4}$	395	0.094	1.07	0.84	385
Weiss	0.24	0.14	1.08	$4.5 \cdot 10^{-4}$	384	$5.2 \cdot 10^{-4}$	389	0.070	1.09	0.68	366
Mare Serenitatis	0.20	0.12	1.21	$5.4 \cdot 10^{-4}$	389	$6.2 \cdot 10^{-4}$	395	0.058	1.11	0.93	397
Mare Nubium	0.20	0.12	1.21	$5.4 \cdot 10^{-4}$	389	$6.2 \cdot 10^{-4}$	395	0.058	1.11	0.88	393

A comparison of T_{tr} and T_{theor} readily demonstrates that the values coincide with an accuracy up to 1 - 1.5% in all cases when cos θ > 0.84, i.e., when the investigated areas are sufficiently far from the edge of the disk. There are four such areas. For the other three areas, we have cos θ = 0.62 - 0.68; their theoretical temperature is noticeably less than that observed. Apparently, the temperature decreases with approach to the edge more slowly than $\sqrt[4]{\cos \theta}$.

This agrees qualitatively with the results of radiometric measurements in the 8 - 13 μ window (Bibl.13, 14). The absolute value of the surface temperature at a subsolar point according to the data given in Table 3 should be close to 395°K. The uncertainty of this value, apparently, does not exceed 10°K. A temperature of 395°K coincides exactly with the theoretical. Pettit and Nicholsen (Bibl.14) found 391°K for the subsolar point, i.e., almost the same; however, Sinton (Bibl.15) gives a value lower by 30°.

TABLE 4

Date	Object	Spectral Width of Exit Slit (at 1.6 μ)	Recording Speed Å/sec	Time Constant sec	Number of Recordings	Zenith Distance	Telescope
3/Oct 1963	Io (I)	0.18	35	20	4	58—50°	ZTE
3/ " 1963	Ganymede (III)	0.18	35	20	4	50—61	[illegible]
1/ " 1964	Callisto (IV)	0.18	35	20	4	27—[illegible]	[illegible]
1/ " 1964	Europa (II)	0.18	35	20	4	30—[illegible]	ZTE
1/ " 1964	Moon	0.18	35	20	4	[illegible]	ZTE
15/ " 1964	Ganymede (III)	0.09	70	4.4	4	27—28	ZTSh
15/ " 1964	Callisto (IV)	0.18	35	20	3	28—30	ZTSh
15/ " 1964	Io (I)	0.09	70	4.4	4	33—38	ZTSh

During the fall of 1963 and 1964, we used a prism spectrometer to record the spectra of the Galilean satellites of Jupiter in the 0.7 - 2.5 μ region./1293 The observations were carried out with the ZTE (125-cm reflector of the Shternberg State Astronomical Institute) and the ZTSh (2.6 reflector of the Crimean Astrophysical Observatory). We used a 0.5 × 0.5 mm lead sulfide photoconductive detector, cooled with solid carbon dioxide. The width of the entrance slit was 0.5 mm and that of the exit slit 2 mm, sometimes 1 mm. A list of the observational data and the recording conditions is given in Table 4, while the single and averaged spectral recordings are given in Figs.6 - 11. A comparison of Figs.6 and 7 shows that, on changing from the zenith telescope ZTE to the ZTSh, we were able to double the resolving power and reduce by a factor of 4 the time

constant at the same signal-to-noise ratio. The resultant gain corresponded about to that expected.

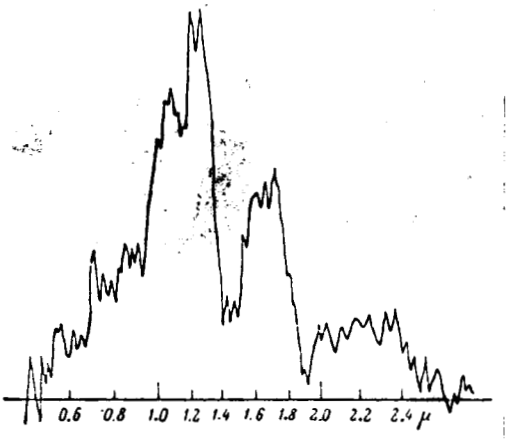

Fig.7 Spectrum of Ganymede in the 0.7 - 2.5 μ Region
(Single Recording)
ZTSh, October 15, 1964, prism spectrometer (LiF),
Δ = 0.09 μ (at 1.6 μ), recording speed 70 Å/sec,
τ = 4.4 sec, z = 28°

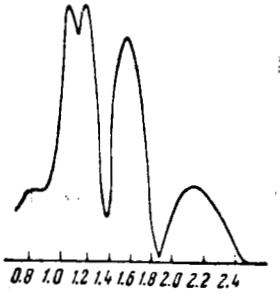

Fig.8 Io, Average of Four Recordings on
October 15, 1964 (ZTSh)
The solar spectrum is given as a broken
line for comparison*

Figure 12 shows the dependence of the geometric albedo of the Galilean satellites on wavelength. In the 0.35 - 0.8 μ region, we used Harris' data, and in the 0.8 - 2.5 μ region we used the spectra shown in Figs.6 - 11. We derived the ratio of the readings in the spectra of the satellites and sun, which were

* There is no broken line in Fig.8. Possible confusion with Fig.9 (translator).

then calibrated so that near 1 μ they fitted into the curve p_λ which is known for the shorter-wave region. In Fig.12 we plotted, in addition to the values of p_λ, the values of the spherical albedo A_λ on the axis of ordinates. For all wavelengths, we used the phase integral q = 0.585 taken by Harris (Bibl.6) for the moon. Since the integral may differ appreciably from this value and vary

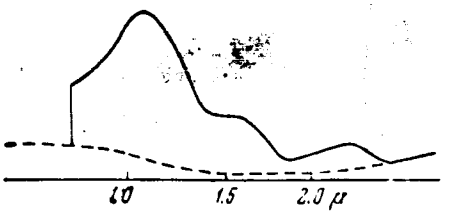

Fig.9 Europa, Average of Four Recordings on October 1, 1964 (ZTE)
The zero-point depends on wavelength as a consequence of weak extraneous exposure

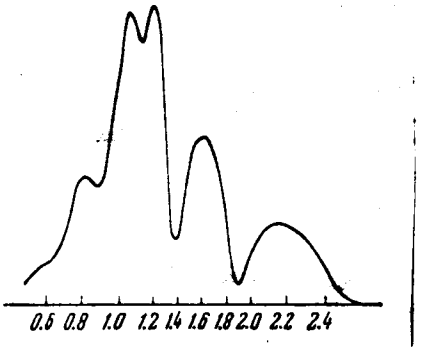

Fig.10 Ganymede, Average of Four Recordings on October 15, 1964 (ZTSh)

with wavelength, the calculated values of spherical albedo and even their relative values are not reliable. The values of the geometric albedo are more reliable, at least their ratios at various wavelengths, since the phase angle is close to zero. The absolute values of p_λ can be distorted by errors in determining the diameter.

It is apparent from a comparison of Figs.12 and 4 that the spectral properties of the surface of the Galilean satellites and of the moon differ substan-

tially. In the 0.35 - 0.8 μ region, all Galilean satellites show, just as /1294 the moon, an increase in reflectance with wavelength. However, in the 1 - 2.5 μ region the reflectance of the Galilean satellites either remains almost constant

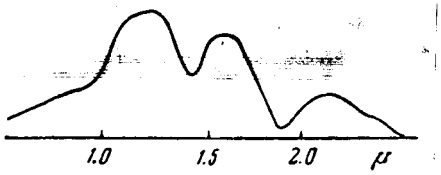

Fig.11 Callisto, Average of Three Recordings on October 15, 1964 (ZTSh)

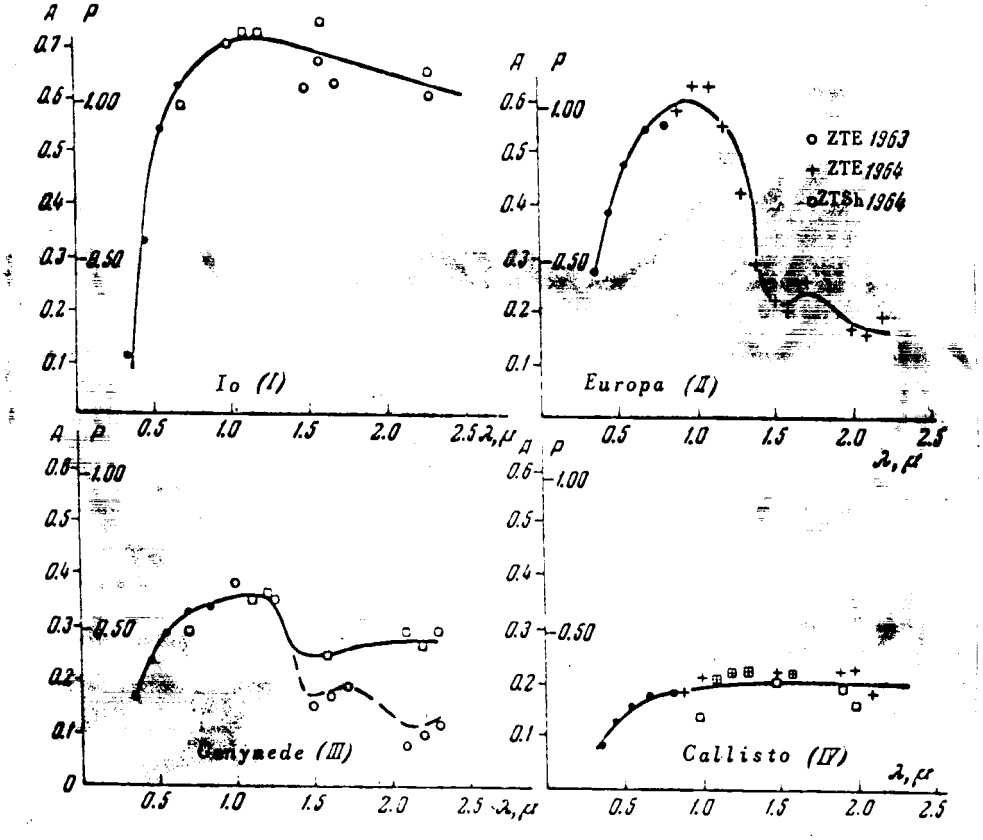

Fig.12 Albedo of the Satellites of Jupiter as a Function of Wavelength

(Io and Callisto) or noticeably diminishes with wavelength (Europa and Ganymede). The albedo of the moon in the 1 - 2.5 μ region, as we saw above, continues to increase with wavelength.

Qualitatively, the dependence of albedo on wavelength in the case of Callisto, and especially in the case of Io, is similar to the curve of the monochromatic albedo of Mars, whereas the spectrum of Europa and Ganymede resembles the spectrum of the polar caps of Mars (Bibl.16) and the rings of Saturn (Bibl.17). This leads to the logical assumption that the surface of both Europa and Ganymede is covered with ice - if not all, at least an appreciable portion of it. Figure 13 shows the time required for evaporation of 1 gm/cm^2 of ice in

TABLE 5

Object	Theoretical Temperature, °K					Measured Temperature, °K (Bibl. 15)	Density gm/cm^3
	A_i	T_e	T_s				
			Average	$\varphi = 0$	$\varphi = 70$		
Io (I)	0.54	121	126	150	117	$\leq$135	3.1
Europa (II)	0.38	130	135	160	125	$\leq$141	3.0
Ganymede (III)	0.27	135	140	166	130	155	1.7
Callisto (IV)	0.17	138	144	171	133	170	1.5

vacuum, as a function of temperature. At a temperature of 125°K, a layer of ice of several kilometers thickness will evaporate in 10^7 years. So that an ice cover of considerable original thickness will not evaporate during the lifetime of the solar system, the temperature must not exceed 130°K. It is interesting to check the agreement between this value and the theoretical and measured (Bibl.18) temperatures of the Galilean satellites. These temperatures are given in Table 5. In this Table, A_i denotes the values of the integrated albedo calculated by means of the curves in Fig.12, T_e is the effective temperature calculated from the condition of thermal equilibrium, and T_s is the surface temperature calculated on the assumption that $\varepsilon = 0.85$. In calculating the theo- /1295
retical temperatures, thermal conductivity was assumed to be negligible.

The measured temperature T_s of Ganymede and Callisto noticeably exceeds T_e.

For T_m and T_e to agree, it is necessary to almost double the diameters of the satellites, which would lead to impossibly small values of the density (see the last column of Table 5). Furthermore, the theoretical temperatures themselves are too high for prolonged conservation of an ice cover in a vacuum. In the presence of an atmosphere, however, this objection is no longer valid. Thus, by assuming the presence of an ice cover on the surface of Europa and Ganymede, we must simultaneously assume the existence of an atmosphere for these satellites. In addition, the difference between the measured and the theoretical temperature can be explained, generally speaking, by an atmosphere. The large absolute albedo values attest to the existence of an atmosphere on Io and Europa.

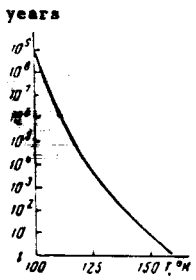

Fig.13 Time Required for Evaporation of 1 gm/cm^2 of Ice as a Function of Temperature

The variations in the brightness of Io, after leaving the shadow of Jupiter, can be interpreted as the effect of a change in albedo produced by the deposition of hoarfrost during darkening and its subsequent sublimation (Bibl.19).

It is not precluded that the depressions in the spectra of Europa and Ganymede can be attributed to some kind of atmospheric absorption; however, we cannot give a specific identification. In any case, CH_4 and NH_3 cannot be responsible for these depressions.

BIBLIOGRAPHY

1. Moroz. V.I.: Astron. Zh., Vol.40, p.144, 1963.

2. Moroz, V.I.: Astron. Zh., Vol.41, p.1108, 1964.

3. Moroz, V.I.: Astron. Zh., Vol.43, 1966 (in Press).

4. Sharonov, V.V.: The Nature of Planets (Priroda planet), Fizmatgiz, 1958.

5. Sytinskaya, N.N.: Astron. Zh., Vol.40, p.1083, 1963.

6. Garris (Harris), D.L.: Planets and Satellites, Edited by G.Kuiper and B.Middlehurst (Planety i sputniki, pod red. Dzh.Koypera i B.Middlkherst). Izd. Inostr. Lit., Moscow, 1963.

7. Kuprevich, N.F.: Astron. Zh., Vol.39, p.1136, 1964; Vol.40, p.889, 1963.

8. Dol'fyus (Dollfuss), A.: Planets and Satellites, Edited by G.Kuiper and B.Middlehurst (Planety i sputniki, pod red. Dzh.Koypera i B.Middlkherst). Izd. Inostr. Lit., Moscow, 1963.

9. Barabashev, N.P. and Chekirda, A.T.: Astron. Zh., Vol.36, p.851, 1959.

10. Shefer, K. and Matossi, F.: Infrared Spectra (Infrakrasnyye spektry). ONTI, Leningrad-Moscow, 1935.

11. van Tassel, R.A. and Salisbury, J.M.: Icarus, Vol.3, p.264, 1964.

12. Troitskiy, V.S.: Astron. Zh., Vol.39, p.73, 1962.

13. Levin, B.Yu.: Astron. Zh., Vol.40, p.1071, 1963.

14. Pettit, E.: Planets and Satellites, Edited by G.Kuiper and B.Middlehurst (Planety i sputniki, pod red. Dzh.Koypera i B.Middlkherst). Izd. Inostr. Lit., Moscow, 1963.

15. Geoffrion, A., Korner, M., and Sinton, W.M.: Lowell Obs. Bull., Vol.5, No.106, 1958.

16. Moroz, V.I.: Astron. Zh., Vol.41, p.352, 1964.

17. Moroz, V.I.: Astron. Zh., Vol.38, p.1080, 1961.

18. Murray, B.C.: Wildey, R.L., and Westphal, J.A.: Astrophys. J., Vol.139, p.986, 1964.

19. Binder, A.B. and Kruikshank, D.P.: Icarus, Vol.3, p.299, 1964.

State Astronomical Institute,
imeni P.K.Shternberg

Received June 17, 1965